The Preparation of Ag Nanoparticles/Graphene Nanocomposites with Polydopamine as Coupling Agent for Enhanced Detection of H₂O₂

Zhi-Min Ma, Bing-Tao Wang, Ke-Ying Cui, Ye Wan, Su-Juan Li[*]

Henan Province Key Laboratory of New Optoelectronic Functional Materials, College of Chemistry and Chemical Engineering, Anyang Normal University, Anyang, 455000, Henan, China
[*]E-mail: lemontree88@163.com

In this paper, a new Ag nanoparticles (AgNPs)/graphene nanocomposites with polydopamine (PDA) as coupling agent was electrochemically synthesized and has been used as electrode modifications for the electrochemical detection of H_2O_2. The structural characterizations clearly showed that small sized and highly dispersed AgNPs were electrodeposited on reduced graphene oxide (RGO) with the help of PDA agent. The obtained AgNPs/PDA/RGO nanocomposites exhibited higher electrocatalytic activities toward reduction of H_2O_2 compared with the AgNPs/RGO composites without involvement of PDA. The AgNPs/PDA/RGO nanocomposites presented excellent electrochemical sensing performance for detection of H_2O_2 with wide linear concentration range, high detection sensitivity, good selectivity and excellent reprodutibility and stability. The successful application of AgNPs/PDA/RGO nanocomposites in human serum samples for the detection of H_2O_2 was also demonstrated.

1. INTRODUCTION

Hydrogen peroxide (H_2O_2), as an small molecule in living organisms, plays significant roles in brain function, such as serving as a signaling molecule in adjusting cellular processes [1-2]. In addition, it can function as a measure of oxidative stress, and the abnormal level of H_2O_2 has been implicated in the initiation and progression of several neurodegenerative disorders, including Parkinson's disease [3-5]. Therefore, sensitive and selective detection of H_2O_2 with accuracy and rapid analysis time are of significant physiological and clinical importance. Among the various analytical techniques for H_2O_2, the determination of H_2O_2 based on electrochemical strategy has been a hot

research topic of high priority [6-8]. Although enzyme based H_2O_2 sensors show advantages of high detection performance, the shortcomings [9], consisting of high price, complicated immobilization procedure, and the weak stability, largely limit their widespread applications. Therefore, development of enzyme-free electrochemical H_2O_2 sensors has been aroused much research interest. While fabrication of nanomaterials with high electrocatalytic properties to promote the electrochemical reaction of H_2O_2 is essential for constructing electrochemical sensors with high performance.

Recently, with the fast development of nanotechnology, various nanomaterials especially noble metal nanoparticles (NPs), such as Au [10,11], Pt [12,13], Pd [14,15], Ag [16,17] etc have been recognized as effective catalysts to improve the electrocatalytic redox kinetics of H_2O_2. Among these nanomaterials, silver nanoparticles (AgNPs) raised great concern due to their unique characters, such as low toxicity, cost-effectiveness, prominent conductivity and durable electrocatalytic activity [16-18]. It is supposed that AgNPs would enhance the electron transfer rate, and its functionality is expected to exhibit promising for construction of H_2O_2 sensors. When AgNPs are modified on conductive substrate, some of their physico-chemical properties, such as size, morphology, and dispersion degree, might affect the electrocatalytic properties [19]. Small sized nanostructures with uniform dispersion is commonly considered to have highly electrocatalytic activities. However, in the process of reduction of metal ions to synthesize AgNPs by chemical or electrochemical methods, metal colloids are prone to aggregate irreversibly to make some of active sites lose their specific function and interact incompletely with target species. To prevent the colloids aggregation, an effective way is exploiting protective species, for example, surfactants, polyelectrolytes and polymers [20-24], which aims at formation of highly dispersed AgNPs and thus efficient electrochemical sensors. Therefore, the achievement of stable and surface dispersible AgNPs for detection of H_2O_2 is extremely desirable.

Polydopamine (PDA) has attracted extensive attention of scientific research since its discovery in 2007 as a novel material [25]. Recently, there are still rapid increasing researches focused on PDA and its derived materials around fabrication and potential applications in areas of environment, sensor, energy, and biomedicine [26-31]. Apart from self-polymerization, dopamine monomer can also be electrochemically deposited onto conductive substrate to form PDA film [32]. After electrochemical overoxidation in alkaline solution, the PDA film is negatively charged and shows permselectivity toward cationic species but not to anionic ones. In addition, the PDA interfaces rich in catechol and amine groups provides the PDA chemical reactivity and abundant nucleation sites for dispersion and stabilization of metal NPs. Based on the above properties, the PDA film has the potential to serve as the coupling agents to AgNPs to improve its performance as electrocatalyst for sensitive analysis of H_2O_2.

In the present work, PDA was exploited as coupling agent on surface of reduced graphene oxide (RGO) for electrodeposition of highly dispersed AgNPs to enhance the electro-reduction of H_2O_2. Here, the dopamine monomer was electrochemically deposited onto RGO surface to form PDA. After overoxidation, the PDA film was negatively charged. Under the electrostatic force and the possible interaction between amine groups of PDA interface and Ag^+ ions in solution, small sized AgNPs with uniform dispersibility can be facilely electrodeposited onto PDA film, resulting in the formation of AgNPs/PDA/RGO nanocomposites. To illustrate the significant role of PDA film, the AgNPs/RGO composites without the participation of PDA was also prepared to compare their

electrocatalytic properties toward H_2O_2 with that of AgNPs/PDA/RGO. Benefiting from the enhanced effect of PDA film, the AgNPs/PDA/RGO nanocomposites showed high performance for amperometric detection of H_2O_2.

2. EXPERIMENTAL SECTION

2.1. Reagents and apparatus

Dopamine, Silver nitrate, hydrogen peroxide and all other chemicals were purchased from aladdin regent Co. and used as received. Graphite oxide (GO) was obtained from Nanjing XFNANO Materials Tech Co., Ltd. A 0.1 M phosphate buffer solutions (PBS, pH 7.0) made from the salts Na_2HPO_4 and KH_2PO_4 were employed as the supporting electrolyte. Unless otherwise stated, water used throughout all experiments was purified with the Millipore system (18.2 MΩ cm).

Scanning electron microscopy (SEM) was conducted by Hitachi SU8010 (Hitachi, Japan) for characterization of surface morphology. Fourier transform infrared (FTIR) spectroscopy (TENSOR37) was performed to characterize the functional groups of GO and PDA/RGO materials. Electrochemical experiments were performed on a CHI 660D electrochemical station (CHI Instruments Inc., USA). A conventional three-electrode system consist of the AgNPs/PDA/RGO modified glassy carbon electrode, a Pt wire and a saturated calomel electrode (SCE) as the working, counter and reference electrodes, respectively.
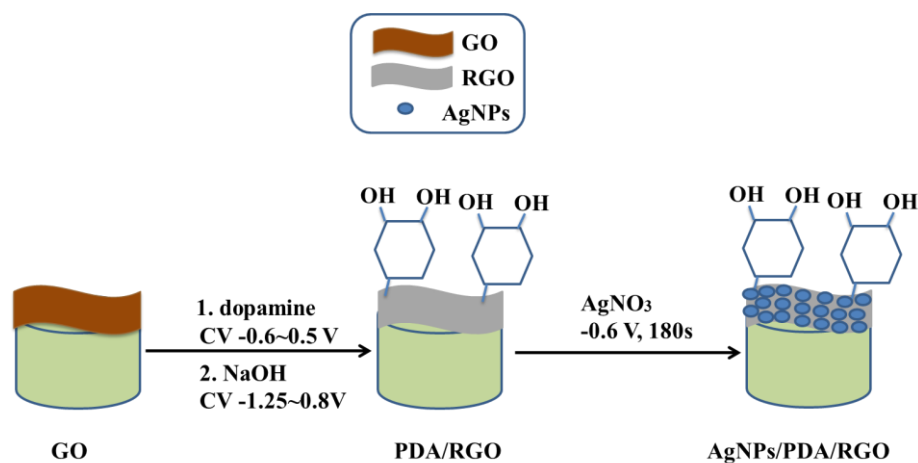
2.2. Preparation of AgNPs/PDA/RGO nanocomposites modified electrode

Before use, a bare GCE with a diameter of 3 mm was polished with 1.0, 0.3 and 0.05 μm alumina powder respectively and then ultrasonically cleaned in water. First, 10 μL 1 mg mL^{-1} GO aqueous dispersion was dispersed onto the polished GCE to obtain the GO modified electrode. Then, the obtained GO modified electrode was immersed into solutions containing the deareated 5 mM dopamine and 60 mM PBS (pH 7.0) and scanned 50 cycles in the potential range from -0.6 to 0.5 V at a scan rate of 100 mV/s. After washed copiously with water, the above electrode was immersed again into PBS solution, and a 40 cycles was performed with the same potential window as above. Last, the modified electrode was switched to a deareated 0.5 M NaOH solution and scanned six cycles from -1.25 to 0.8 V at a scan rate of 50 mV/s to overoxidize the formed PDA film. After rinsed with water, AgNPs was further modified by electrodeposition under a constant potential of -0.6 V in electrolyte solutions of 0.1 M KNO_3 containing 5 mM $AgNO_3$ for an optimal time of 180 s. This electrode was denoted as AgNPs/PDA/RGO modified electrode. For comparison, AgNPs/RGO modified electrode was prepared using the same procedures as above except for electrodeposition of PDA film and its overoxidation.

3. RESULTS AND DISCUSSION

3.1. Synthesis and characterization of modified electrodes

In the current study, a simple and green electrochemical synthesis strategy was used to prepare AgNPs/PDA/RGO nanocomposites. The whole procedures for preparation of the AgNPs/PDA/RGO nanocomposites are schematically illustrated in Scheme 1. First, the dopamine monomer was electrodeposited onto GO modified electrode by CV technique. During this process, PDA film was covered onto electrode surface, meanwhile, the GO was partly reduced to RGO. After overoxidation in NaOH solution through CV method, the reduction degree of GO is supposed to increase, and the overoxidized PDA film is reported to behave like a permselective membrane to selectively transport cationic species but inhibit anionic ones, due to its negative charge [32-35]. When the PDA/RGO composites was subsequently immersed into silver precursor, under the electrostatic force and the possible interaction between amine groups of PDA film and Ag^+ ions in solution, small sized AgNPs with uniform dispersion can be facilely electrodeposited onto PDA film, resulting in the formation of AgNPs/PDA/RGO nanocomposites. During the electrochemical reduction of Ag^+ to Ag^0, PDA film acts as not only a stabilizer to disperse Ag nanocrocrystals but also provides plentiful nucleation sites for the growing of AgNPs with aboundant loading and good dispersity.

Scheme 1. Schematic illustration of the procedures for preparing the AgNPs/PDA/RGO nanocomposites.

3.1.1 FTIR analysis

As shown in Fig. 1, the line b is the FTIR spectrum of GO. The GO characteristic bands are present at 1730 cm^{-1} (C=O stretching in carboxylic acid and carbonyl moieties), 1410 cm^{-1} (C-OH stretching) and 1055 cm^{-1} (C-O stretching) [30,36]. The line c is the FTIR spectrum of PDA/RGO composites. Obviously, the characteristic absorption bands of oxygen functionalities, such as the bands at 1730 cm^{-1} and 1055 cm^{-1} , are decreased in some extent compared to GO, indicating the partly reduction of GO in PDA/RGO composites. Meanwhile, new bands are observed at 1518 cm^{-1} (N-H shearing vibration) [28] and 1577 cm^{-1} (the benzene skeleton vibration of PDA) [37], which confirms success in obtaining PDA functionalized RGO.
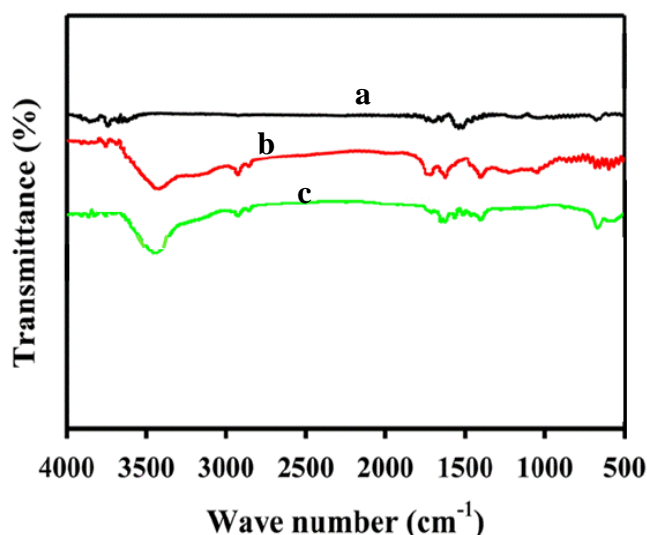
Figure 1. FTIR spectrum of PDA (a), GO (b) and PDA/RGO (c) modified electrode.

3.1.2 Morphology characterization

The SEM images of electrodes modified with materials of GO (a), PDA/RGO (b), AgNPs/PDA/RGO (c) and AgNPs/RGO (d) were given in Fig. 2. It can be seen that the GO (Fig. 2a) shows representative structure with wrinkled nanosheets [28,38,39]. After modification with PDA molecules, a thin layer of PDA films is covered onto RGO surface (Fig. 2b). When AgNPs are further electrodeposited on electrode, it is observed to be homogeneously dispersed on PDA/RGO surface without any aggregation (Fig. 2c). The AgNPs sizes have a diameter ranging from 10 to 20 nm, with an average diameter of about 15 nm. In contrast, in the absence of PDA, the AgNPs formed by the same electrodeposition method have no uniform sizes and aggregation can be distinctly found. In addition, the sizes of AgNPs increased significantly to even 100 or 200 nm (Fig. 2d). These results suggest that PDA plays a vital role in the formation of small sized and uniformly dispersed AgNPs. The thin layer of PDA film on RGO is utilized as coupling agent that acts to adsorb and bind the Ag^+ through the electrostatic force between Ag^+ and the negatively charged PDA film and the possible interaction between amine groups of PDA and Ag^+ ions. These interactions restrict the particle growth during reduction, resulting in high dispersion of AgNPs [40]. The SEM images have verified that AgNPs deposited on PDA/RGO surface can produce small sized, uniform and intensive distribution of AgNPs. Here, the role of PDA on RGO surface is similar with poly(ionic liquid) functionalized graphene sheets in the formation of AgNPs [20].
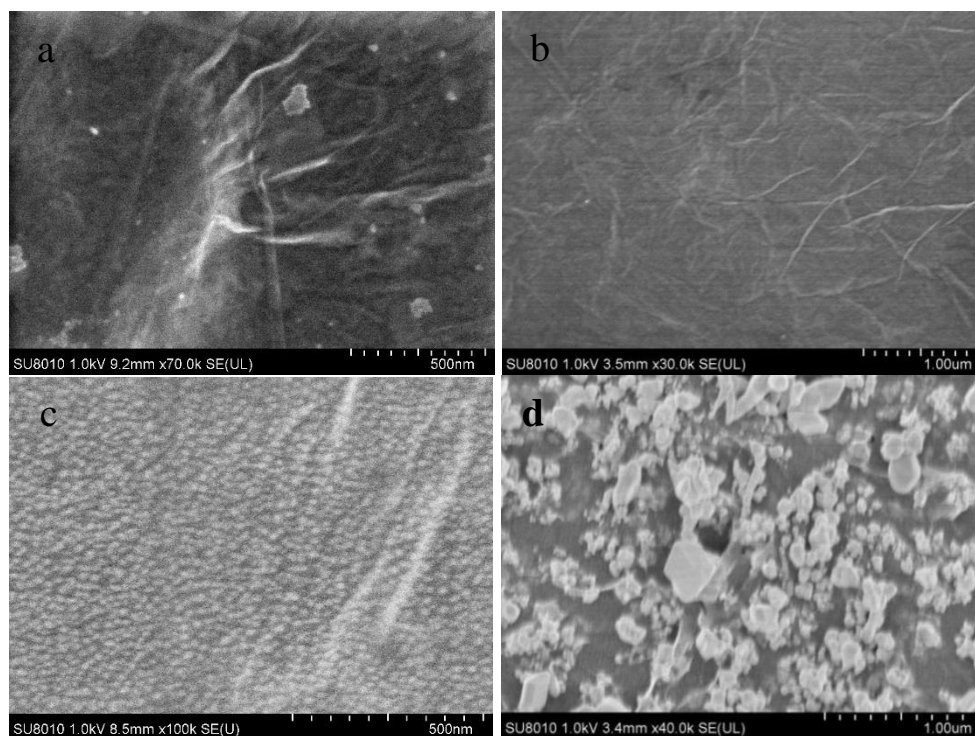
Figure 2. SEM images of electrode modified with materials of GO (a), PDA/RGO (b), AgNPs/PDA/RGO (c) and AgNPs /RGO (d).

3.1.3 EIS characterization

EIS was used to study the electric conductivity of the electrodes modified with each layer of materials, through the survey of the charge-transfer resistance (R_{ct}) at the interface of electrode and electrolyte. Fig. 3 presents the EIS plots measured in 5 mM $[Fe(CN)_6]^{3-}/^{4-}$ with 0.1 M KCl as supporting electrolyte for the bare GCE and GO, PDA/RGO, AgNPs/PDA/RGO modified electrodes. In Nyquist plots, the semicircle diameter at high frequency reports the kinetics of electron transfer for $[Fe(CN)_6]^{3-}/^{4-}$ at the interface of electrode, and the diameter is equivalent to the R_{ct} value [41]. As observed, upon modification of GO nanosheets on electrode surface, a significant largest R_{ct} value appeared due to the low conductivity of GO and the inhibition effect toward $Fe(CN)_6^{3-}/Fe(CN)_6^{4-}$ arising from plenty of negatively charged oxygen-containing groups on GO surface. With the subsequent electrodeposition of PDA films, the R_{ct} value of PDA/RGO modified electrode significantly decreased, probably because of the prominent electrical conductivity of the formed PDA films and the restorative electronic structure of RGO material caused by partially electrochemical reduction of GO [36]. Finally, the further decoration of AgNPs to form AgNPs/PDA/RGO modified electrode, an obvious decrease of R_{ct} value was observed by comparison with PDA/RGO modified electrode, suggesting that the introduction of AgNPs indeed enhance electron transfer efficiency of AgNPs/PDA/RGO nanocomposites. These results indicate the feasibility of the AgNPs/PDA/RGO nanocomposites for designing a highly efficient electrochemical sensor.
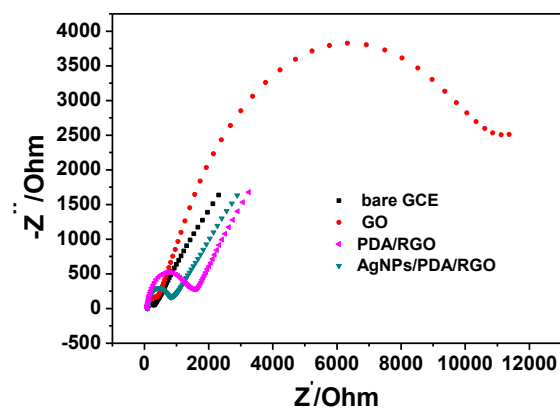
Figure 3. The EIS plots of bare electrode and GO, PDA/RGO, AgNPs/PDA/RGO modified elctrodes in 5 mM $Fe(CN)_6^{3-/4-}$ and 0.1 mol/L KCl solution in the frequency range of 10^5-0.01 Hz.

3.2. Electrocatalytic performance of AgNPs/PDA/RGO nanocomposites toward H_2O_2

The electrocatalytic performance of AgNPs/PDA/RGO nanocomposites toward reduction of H_2O_2 was assessed by comparing its CV response with electrodes such as the bare electrode, PDA/RGO and AgNPs/RGO modified electrodes in 0.1 M pH 7.0 PBS with absence (black lines) and presence (red lines) of 5 mM H_2O_2. As shown in Fig.4, at the bare electrode (Fig.4a), the reduction of H_2O_2 starts from a potential of about -0.45 V from the comparison of CV curves in blank solution and analyte of H_2O_2, and the cathodic current of H_2O_2 is very small. While at PDA/RGO modified electrode (Fig.4b), a more positive onset potential for reduction of H_2O_2 presents at -0.2 V, in addition, an enhanced cathodic current is found. This is ascribed to the good electrical conductivity and well electrocatalytic activity of PDA/RGO materials. For AgNPs/PDA/RGO modified electrode (Fig.4c), it can be observed that the onset potential for reduction of H_2O_2 starts from -0.16 V, which is more positive than that of PDA/RGO modified electrode. Moreover, the cathodic current of H_2O_2 at AgNPs/PDA/RGO is obviously much larger than that of PDA/RGO modified electrode. Such results indicate the important role of AgNPs in AgNPs/PDA/RGO nanocomposites for performing excellent electrocatalytic properties toward H_2O_2. To illustrate the significant role of PDA film in preparing such highly efficient AgNPs/PDA/RGO based H_2O_2 sensor, AgNPs was directly electrodeposited onto RGO surface without the participation of PDA to obtain AgNPs/RGO modified electrode for comparison. As displayed in Fig.4d, the reduction of H_2O_2 at AgNPs/RGO modified electrode starts from -0.23 V, more negative than -0.16 V for AgNPs/PDA/RGO electrode, suggesting the superior electrocatalytic activities of AgNPs/PDA/RGO nanocomposites. The possible reason can be ascribed to the coupling effect of PDA films for facile deposition of AgNPs with small particle size and high dispersibility. The highly dispersed and small sized AgNPs in AgNPs/PDA/RGO composites is beneficial for electrocatalytic reduction of H_2O_2 due to more active sites available.
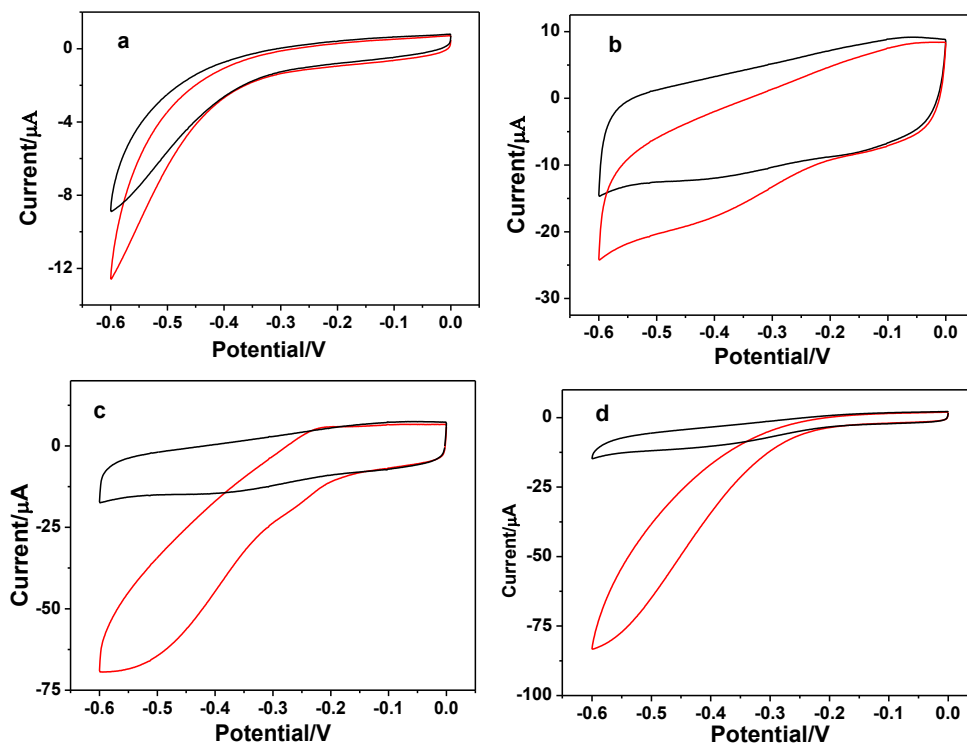
Figure 4. (a) CV responses of the bare electrode (a), PDA/RGO (b), AgNPs/PDA/RGO (c) and AgNPs/RGO (d) modified elctrodes with the absence (black lines) and the presence (red lines), respectively, of 5 mM H_2O_2 in 0.1 M PBS (pH 7.4) at a scan rate of 50 mV s^{-1}.

To further evaluate the ratio of each components in AgNPs/PDA/RGO nanocomposites on H_2O_2 catalytic performance and confirm its prominent electrocatalytic activity, amperometric curve of different electrodes upon addition of 50 µM H_2O_2 was recorded. As seen from Fig. 5, the faradic currents of H_2O_2 at electrodes of untreated and PDA/RGO, AgNPs/PDA/RGO, AgNPs/RGO modified electrodes are found to be 0.023, 0.094, 3.920 and 2.784 µA, respectively. The presence of PDA film and AgNPs gives a current of 1.136 and 3.826 µA, respectively, for H_2O_2 reduction, from the height difference of current between the above adjacent electrodes. Faradic currents obtained on AgNPs/PDA/RGO composites are the largest among all of electrodes, which shows potentials of AgNPs/PDA/RGO nanocomposites in constructing a highly sensitive H_2O_2 sensor. In addition, it can be observed that different electrodes have different starting currents. While the starting current in the amperometric curves is related to the current response of electrode in blank PBS solutions. Therefore, the different starting currents for the above four electrodes suggest that the current response of the above four electrodes in blank PBS solutions is different. This result is consistent with CV results observed in Fig 4.
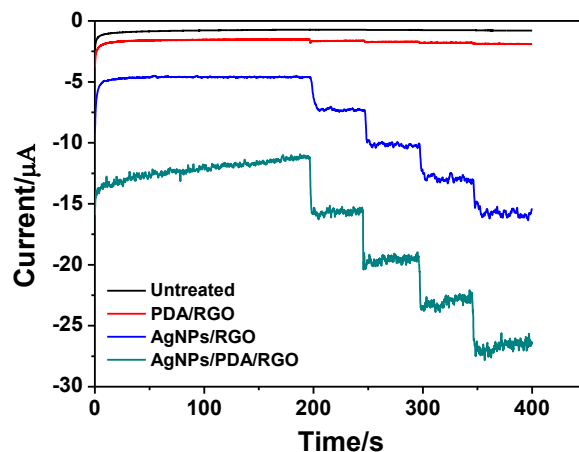
Figure 5. Amperometric responses of the above four electrodes for successive additions of 50 μM H_2O_2 into 0.1 M PBS (pH 7.0) solution at an applied potential of -0.3 V.

The effect of deposition time for AgNPs in preparing AgNPs/PDA/RGO nanocomposites on CV responses of H_2O_2 was studied to maximize the detection sensitivity, the results of which is presented in Fig. 6. The cathodic currents of H_2O_2 increase apparently with increasing the deposition time from 60 to 120 s. With the further increase of deposition time from 120 to 240 s, the cathodic currents increase slowly on the contrary, indicating the low utilization efficiency of AgNPs at longer deposition time though more amount of AgNPs deposited. Therefore, from the point of view of low-cost and high catalytic efficiency, 120 s was used for deposition of AgNPs to prepare AgNPs/PDA/RGO nanocomposites.
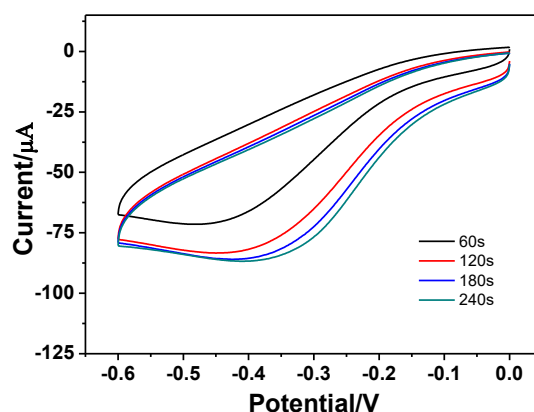

Figure 6. The effect of deposition time (60, 120, 180, 240 s) for AgNPs in preparing AgNPs/PDA/RGO nanocomposites on CV responses of 5 mM H_2O_2.

Fig. 7 shows the CVs of AgNPs/PDA/RGO modified electrode in different concentrations of H_2O_2 with 0.1 M PBS as electrolyte. Obviously, the cathodic current of H_2O_2 at -0.5 V is found to be proportional to its concentration (inset) with a linear regression equation of $I(\mu A)=-14.9252-71.5543C(mM)$ (R=0.9990), which indicates the potential prospect for the subsequent quantitative analysis.
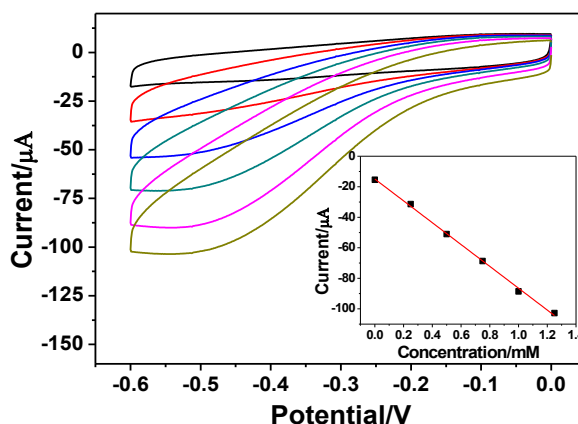
Figure 7. CV responses of AgNPs/PDA/RGO modified electrode in different concentrations (from inner to outer: 0，0.25，0.5，0.75，1.0，1.25 mM) of H_2O_2 with 0.1 M PBS as electrolyte; The inset is the relationship between the cathodic current at -0.5 Vand concentration of H_2O_2.

3.3. Amperometric responses of the AgNPs/PDA/RGO nanocomposites toward H_2O_2

Amperometric method was explored for electrochemical determination of H_2O_2. The current-time curve was conducted to measure the electrochemical sensing performance of AgNPs/PDA/RGO electrode toward H_2O_2. Firstly, applied potential possibly affecting the current response of the fabricated enzyme-free H_2O_2 sensor was optimized. Fig. 8a shows the typical amperometric currents of AgNPs/PDA/RGO electrode to successive additions of 50 μM H_2O_2 under different potentials. It is obvious that the current responses of 50 μM H_2O_2 increase from -0.2 to -0.3 V and level off with the further negative shift of applied potential to -0.4 V. As well known, more negative potential will lead to poor selectivity for H_2O_2 reduction [35], thus, -0.3 V is selected as optimal detection potential.

Fig. 8b displays the amperometric currents of AgNPs/PDA/RGO electrode to successive additions of various concentrations of H_2O_2 into 0.1 M PBS (pH 7) under detection potential of -0.3 V. Amperometric reduction currents of H_2O_2 increasing stepwise with its concentration are obtained, with a response time of <3 s, suggesting a rapid response and high sensitivity of AgNPs/PDA/RGO nanocomposites to H_2O_2. Fig. 8c shows the response currents of AgNPs/PDA/RGO electrode as a function of H_2O_2 concentration. The obtained calibration curve of AgNPs/PDA/RGO electrode gives the following equation I(μA)=-7.7162-0.0099C (μM) with a correlation coefficient of 0.9975. The response to H_2O_2 exhibits a wide linear range with concentration from 5 μM to 9.97 mM with a detection sensitivity of 140 μA mM^{-1} cm^{-2} (9.9 μA mM^{-1}). When the concentration is above 9.97 mM, its will deviate from the linear range. The possible reason is ascribed to higher concentration of H_2O_2 above than 9.97 mM will alter its adsorption mechanism on interface of AgNPs/PDA/RGO nanocomposites, leading to lower electrochemical reaction kinetics. The detection limit of AgNPs/PDA/RGO based H_2O_2 sensor is estimated to be 0.68 μM.

Table 1. Comparison of the analytical performances of various Ag based hybrid nanomaterials toward H_2O_2 detection

Electrode materials	Potential (V)	Sensitivity ($\mu A\ mM^{-1}\ cm^{-2}$)	Linear range (mM)	LOD (μM)	Ref.
3D-rGO/AgNP	-0.3 *vs.*Ag/AgCl	419.7	0.016–27	6.8	16
PDA–Ag	-0.3 *vs.* SCE	6.79 $\mu A\ mM^{-1}$	0.092–20	1.97	17
AgNPs/rGO	-0.3 *vs.*Ag/AgCl	–	0.1–100	3.6	18
AgNP–PmPD	-0.9 *vs.* SCE	–	0.1–10	0.88	21
Ag/ZIF–8	-0.6 *vs.*Ag/AgCl	398.47	0.02–5, 5.5–10	6.2	42
Hb/Ag NPs	-0.2 *vs.*Ag/AgCl	2.83 $\mu A\ mM^{-1}$	5×10^{-4}–20	0.42	43
ERGO–Ag	-0.5 *vs.*Ag/AgCl	–	0.0016–9	1.6	44
N–graphene–AgND	-0.4 *vs.*Ag/AgCl	88.47	0.1–80	0.26	45
ERGO–AgNCs	-0.5 *vs.*Ag/AgCl	183.5	0.02–10	3	46
Ag@SiO$_2$@Ag	-0.2 *vs.* SCE	56.07	0.005−24	1.7	47
Ag nanowire array	-0.2 *vs.* SCE	26.6	0.1–3.1	29.2	48
Ag@BSA	-	101.3	0.005–1.5	0.16	49
AgNPs/PDA/RGO	-0.3 *vs.* SCE	140 (9.9 $\mu A\ mM^{-1}$)	0.005–9.97	0.68	This work

The comparison of the analytical performance of AgNPs/PDA/RGO based H_2O_2 sensor with other Ag based hybrid nanomaterials previously reported is shown in Table 1, in terms of detection potential, sensitivity, linear concentration range and limit of detection (LOD). As can be seen, the present sensor has better or comparable characteristics than most of the previously reported H_2O_2 sensors given in Table 1. The linear range of AgNPs/PDA/RGO composites is only lower than that of Hb/AgNPs [43] based enzymatic and Ag@SiO$_2$@Ag [47] based nonenzymatic H_2O_2 sensors, but is wider than most of the other sensors. The detection sensitivity and LOD value obtained in the present work is also on the top of performance among various Ag based hybrids. In addition, the relatively positive reduction potential applied has the possibility to eliminate interference of reductive substance possibly affecting the reduction current of H_2O_2.

From the above comparison, it can be concluded that the AgNPs/PDA/RGO nanocomposites can be utilized as an efficient platform for H_2O_2 detection with wide linear range, low detection limit, and high sensitivity and selectivity. The outstanding electrocatalytic activity of AgNPs/PDA/RGO nanocomposites can be ascribed to the following reasons: firstly, the coupling effect of PDA film makes small sized AgNPs dispersed uniformly on RGO surface, thus offering aboundant active sites and promoting the adsorption of H_2O_2 on electrode surface; secondly, the combination of conductive PDA/RGO support with metal AgNPs to form highly conductive AgNPs/PDA/RGO composites, enhance distinctly electron transfer between modified electrode and electrolyte.
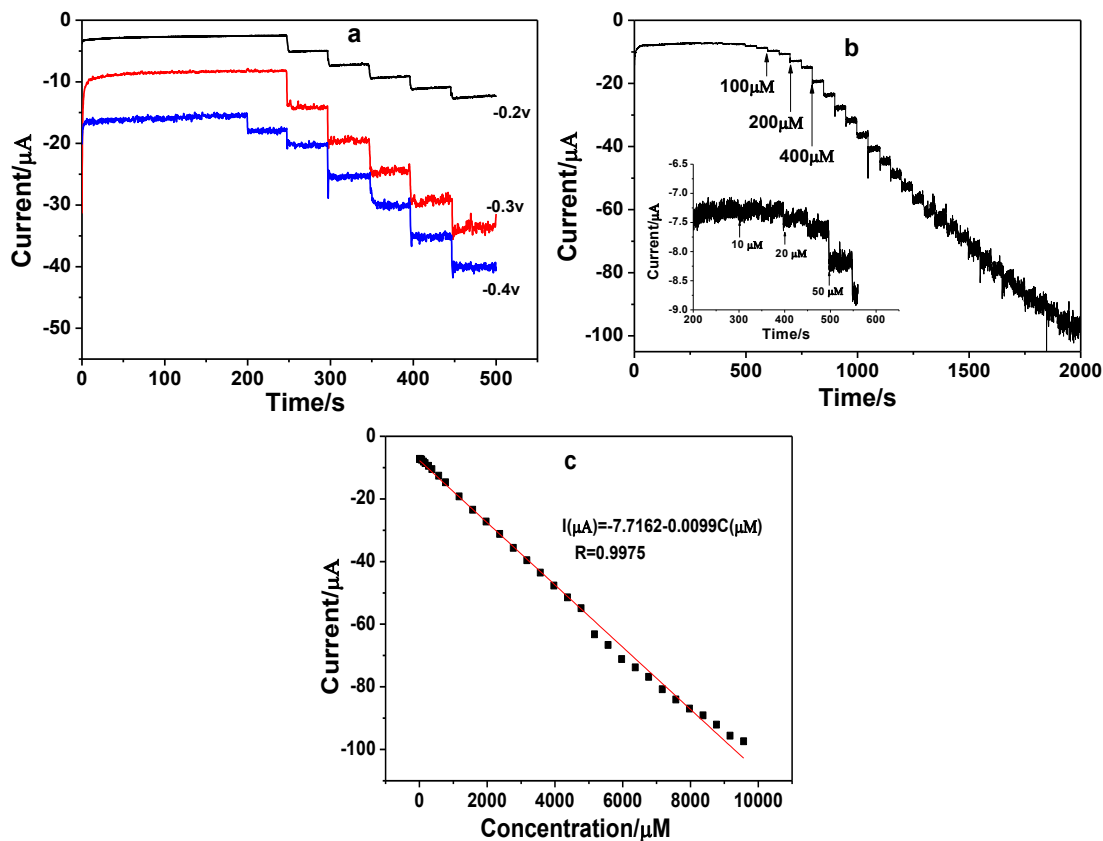
Figure 8. Detection of H_2O_2 in 0.1 M PBS (pH7.0) solution using the AgNPs/PDA/RGO electrode: (a) Amperometric responses of AgNPs/PDA/RGO electrode to successive additions of 50 μM H_2O_2 at the applied potentials of -0.2, -0.3 and -0.4 V, respectively; (b) Amperometric responses of AgNPs/PDA/RGO electrode (holding at -0.3 V) upon addition of H_2O_2 to increasing concentrations; (c) The calibration curve of the present sensor with the data obtained from fig.8b.

3.4. Reproducibility, repeatability, stability, and anti-interference ability of the AgNPs/PDA/RGO nanocomposites modified electrode

The reproducibility, repeatability and stability are important parameters for assessing the sensor performance. The reproducibility of the prepared AgNPs/PDA/RGO electrode was investigated from its current response to 100 μM H_2O_2 using six electrodes prepared separately using the same methods. A 3.26% of relative standard deviation (RSD) was obtained, indicating an acceptable reproducibility of the fabrication method. The steady-state current response of 100 μM H_2O_2 for consecutive measurement of 6 times was recorded at the same electrode to examine the repeatability. The obtained RSD was only 2.28%, suggesting excellent repeatability of the AgNPs/PDA/RGO electrode. The storage stability of the AgNPs/PDA/RGO electrode was evaluated by determining current response of 100 μM H_2O_2 within a month. If not in use, the modified electrode was stored in room temperature. The results suggest that a 87% of its initial current was retained after intermittent usage for one month. Therefore, we can conclude that the AgNPs/PDA/RGO electrode exhibited good stability.
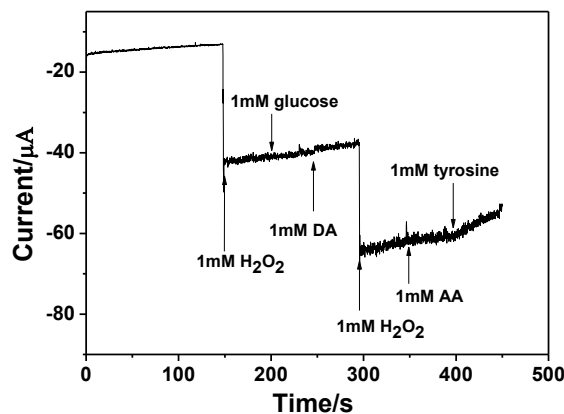
Figure 9. Amperometric responses of the AgNPs/PDA/RGO electrode to successive additions of 1 mM H_2O_2, 1 mM glucose, 1 mM DA, 1 mM H_2O_2, 1 mM AA and 1 mM tyrosine in 0.1 M PBS at -0.3 V.

The anti-interference property of the AgNPs/PDA/RGO electrode was investigated by comparing the current signals of H_2O_2 and possible interferent in physiological samples. Fig. 9 shows the amperometric responses of the AgNPs/PDA/RGO electrode to successive additions of 1 mM H_2O_2, 1 mM glucose, 1 mM dopamine (DA), 1 mM H_2O_2, 1 mM ascobic acid (AA) and 1 mM tyrosine in 0.1 M PBS at -0.3 V. As observed, a remarkable H_2O_2 signal was found compared to the other interferent e.g. glucose, DA, AA and tyrosine, and the presence of interference species nearly does not influence the current signal of added H_2O_2. Compared to H_2O_2, all interferent generated current responses less than 20%. Thus, the proposed AgNPs/PDA/RGO electrode exhibited outstanding selectivity.

3.5. Analysis of H_2O_2 in human serum samples

For evaluating the feasibility of the present method in real samples, electrochemcial detection of H_2O_2 in human serum using the AgNPs/PDA/RGO electrode was conducted. The serum samples were first ten-fold diluted with 0.1 M pH 7.0 PBS, and then spiked with different concentrations of H_2O_2. 15.28 μM of H_2O_2 was found in the human serum samples. The recovery of H_2O_2 spiked into the human serum samples was measured with standard addition method. The determication results is shown in Table 2. Obviously, the recovery and RSD results are acceptable, revealing the feasibility of the present method for electrochemcial detection of H_2O_2 in real samples.

Table 2. Amperometric determination of H_2O_2 in human serum samples by the proposed method.

Original amount (μM)	Spiked amount (μM)	Detected amount (μM)	RSD (%)	Recovery(%)
15.28	10.00	24.48	4.29	92.00
15.28	20.00	36.17	5.16	104.4
15.28	30.00	43.10	3.84	92.73

4. CONCLUSIONS

We report here a simple electrochemical strategy for preparing AgNPs/PDA/RGO nanocomposites. In these nanocomposites, the PDA plays a crucial role in obtaining small sized and highly dispersed AgNPs, which shows an enhanced electrocatalytic activities for reduction of H_2O_2. As an electrochemical sensing platform for H_2O_2, the performance of AgNPs/PDA/RGO nanocomposites was studied by different electrochemical techniques. The results showed that the AgNPs/PDA/RGO nanocomposites can be used as an enzyme-free H_2O_2 sensor with high detection, good sensitivity and low limit of detection. The linear concentration range of H_2O_2 was from 0.005 to 9.97 mM with a low detection limit of 0.68 μM. In addition, common biological substances did not interfere with the electrochemical signal of H_2O_2. The successful application of AgNPs/PDA/RGO nanocomposites for determination of H_2O_2 is also demonstrated in human serum samples. The present work shows that the metal catalysts/graphene composites prepared with PDA as coupling agent represent a class of high efficient materials with electrocatalytic activities for enzyme-free detection of H_2O_2 for practical application.

References

1. W. Chen, S. Cai, Q.Q. Ren, W. Wen and Y.D. Zhao, *Analyst*, 137 (2012) 49.
2. S.Z. Bas, C. Cummins, D. Borah, M. Ozmen and M.A. Morris, *Anal. Chem.*, 90 (2018) 1122.
3. L.R. Wilson, S. Panda, A.C. Schmidt and L.A. Sombers, *Anal. Chem.*, 90 (2018) 888.
4. M. Asif, H. Wang, S. Dong, A. Aziz, G. Zhang, F. Xiao and H. Liu, *Sens. Actuators B*, 239 (2017) 243.
5. S.K. Maji, S. Sreejith, A.K. Mandal, X. Ma and Y. Zhao, *ACS Appl. Mater. Interfaces*, 6 (2014)13648.
6. C. Cheng, C. Zhang, X. Gao, Z. Zhuang and C Du, *Anal. Chem.*, 90 (2018)1983.
7. B. Sherino, S. Mohamad, S.N.A. Halim, N.S.A. Manan and W. Chen, *Sens. Actuators B*, 254 (2018) 1148.
8. Z.L. Wu, C.K. Li, F. Zhu, S. Liao, J.G. Yu, H. Yang and X.Q. Chen, *Sens Actuators B*, 253 (2017) 949.
9. X. Chen, G. Wu, Z. Cai, M. Oyama and X. Chen, *Microchim. Acta*, 181(2014) 689.
10. S.J. Li, Y.F. Shi, L. Liu, L.X. Song, H. Pang and J.M. Du, *Electrochim. Acta*, 85(2012) 628.
11. M.R. Zhang, X.Q. Chen and G.B. Pan, *Sens. Actuators B*, 240 (2017)142.
12. L. Xing, Q. Rong and Z. Ma, *Sens. Actuators B*, 221 (2015) 242.
13. K. Ye, D. Zhang, H. Zhang, K. Cheng, G. Wang and D. Cao, *Electrochim. Acta*, 178 (2015) 270.
14. M. Sookhakian, E. Zalnezhad and Y. Alias, *Sens. Actuators B*, 241 (2017) 1.
15. M. Han, S. Liu, J. Bao and Z. Dai, *Biosens. Bioelectron.*, 31 (2012) 151.
16. X. Lou, C. Zhu, H. Pan, J. Ma, S. Zhu, D. Zhang and X. Jiang, *Electrochim. Acta*, 205 (2016) 70.
17. A.J. Wang, Q.C. Liao, J.J. Feng, Z.Z. Yan and J.R. Chen, *Electrochim. Acta*, 61 (2012) 31.

18. Q. Li, X. Qin, Y. Luo, W. Lu, G. Chang, A.M. Asiri, A.O. Al-Youbi and X. Sun, *Electrochim. Acta*, 83 (2012) 283.
19. X. Niu, L. Shi, J. Pan, F. Qiu, Y. Yan, H. Zhao and Lan M, *Electrochim. Acta*, 199 (2016) 187.
20. Q. Wang and Y. Yun, *Microchim. Acta*, 180 (2013) 261.
21. Z. Wu, S.Yang, Z. Chen, T. Zhang, T. Guo, Z. Wang and F. Liao, *Electrochim, Acta*, 98 (2013) 104.
22. S. Liu, J. Tian, L. Wang and X. Sun, *Carbon*, 49 (2011) 3158.
23. S. Liu, L. Wang, J. Tian, Y. Luo, X. Zhang and X. Sun, *J. Colloid Interf. Sci.*, 363 (2011) 615.
24. X. Qin, W. Lu, Y. Luo, G. Chang, A.M. Asiri and A.O. Al-Youbi and X. Sun, *Analyst*, 137 (2012) 939.
25. H. Lee, S.M. Dellatore, W.M. Miller and P.B. Messersmith, *Science*, 318 (2007) 426.
26. Z. Yang, Y. Wu, J. Wang, B. Cao and C.Y. Tang, *Environ. Sci. Technol.*, 50 (2016) 9543.
27. C. Zhang, H.C. Yang, L.S. Wan, H.Q. Liang, H. Li and Z.K. Xu, *ACS Appl. Mater. Interfaces*, 7 (2015) 11567.
28. X. Zheng, J. Zhang, J. Wang, X. Qi, J.M. Rosenholm and K. Cai, *J. Phys. Chem. C*, 119 (2015) 24512.
29. S. Zhang, Y. Zhang, G. Bi, J. Liu, Z. Wang, Q. Xu, H. Xu and X. Li, *J. Hazard. Mater.*, 270 (2014) 27.
30. J. Miao, H. Liu, W. Li and X. Zhang, *Langmuir*, 32 (2016) 5365.
31. C. Li, Y. Zhao, L. He, R. Mo, H. Gao, C. Zhou, P. Hong, S. Sun and G. Zhang, *Chem. Commun.*, 54 (2018) 3122.
32. T. Łuczak, *Electrochim. Acta*, 53 (2008) 5725.
33. G.H. Choi, D.K. Rhee, A.R. Park, M.J. Oh, S. Hong, J.J. Richardson, J. Guo, F. Caruso and P.J. Yoo, *ACS Appl. Mater. Interfaces*, 8 (2016) 3250.
34. H.Y. Chang, D.I. Kim and Y.C. Park, *Electroanalysis*, 18 (2006) 1578.
35. R. Li, X. Liu, W. Qiu and M. Zhang, *Anal. Chem.*, 88 (2016) 7769.
36. S.J. Li, Y. Xing, D.H. Deng, M.M. Shi and P.P. Guan, *J. Solid State Electrochem.*, 19 (2015) 861.
37. Y. Cheng, S. Zhang, N. Kang, J. Huang, X. Lv, K. Wen, S. Ye, Z. Chen, X. Zhou and L. Ren, *ACS Appl. Mater. Interfaces*, 9 (2017) 19296.
38. L. Fu, G. Lai, B. Jia and A. Yu, *Electrocatalysis*, 6 (2015) 72.
39. R. Mo, X. Wang, Q. Yuan, X. Yan, T. Su, Y. Feng, L. Lv, C. Zhou, P. Hong, S. Sun, Z. Wang and C. Li, *Sensors*, 18 (2018) 1986.
40. X. Bo, J. Bai, B. Qi and L. Guo, *Biosens. Bioelectron.*, 28 (2011) 77.
41. A. Yari and S. Derki, *Sens. Actuators B*, 227 (2016) 456.
42. A. Samadi-Maybodi, S. Ghasemi and H. Ghaffari-Rad, *Electrochim. Acta*, 163 (2015) 280.
43. L. Jiang, J. Hu and J.S. Foord, *Electrochim. Acta*, 176 (2015) 488.
44. B. Zhao, Z. Liu, W. Fu and H. Yang, *Electrochem. Commun.*, 27 (2013) 1.
45. M.T. Tajabadi, W.J. Basirun, F. Lorestani, R. Zakaria, S. Baradaran, Y.M. Amin, M.R. Mahmoudian, M. Rezayi and M. Sookhakian, *Electrochim. Acta*, 151 (2015) 126.
46. L. Zhong, S. Gan, X. Fu, F. Li, D. Han, L. Guo and L. Niu, *Electrochim. Acta*, 89 (2013) 222.
47. H. Hao, Q. Sheng and J. Zheng, *Colloids and Surfaces A: Physicochem. Eng. Aspects*, 518 (2017) 124.
48. E. Kurowska, A. Brzózka, M. Jarosz, G.D. Sulka and M. Jaskuła, *Electrochim. Acta*, 104 (2013) 439.
49. Q. Liu, T. Zhang, L. Yu, N. Jia and D.P. Yang, *Analyst*, 138 (2013) 5559.